Marie Skłodowska-Curie (MSCA) – Innovative Training Networks (ITN)

H2020-MSCA-ITN European Training Networks

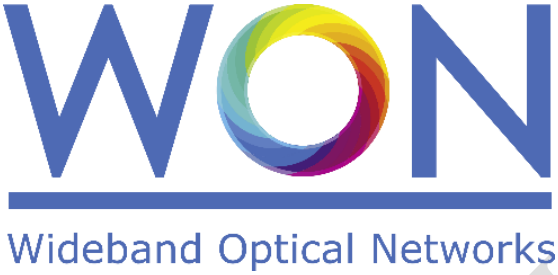

Wideband Optical Networks [WON]

Grant agreement ID: 814276

WP3 – In-line component design

Deliverable D3.3 Implementation and characterisation of the Raman and Bi-doped designs

This project has received funding from the European Union's Horizon 2020 research and innovation programme under the Marie Skłodowska-Curie grant agreement 814276.

Document Details

Work Package	WP3- In-line component design
Deliverable number	D3.3
Deliverable Title	Implementation and characterisation of the Raman and Bi-doped designs
Lead Beneficiary:	Aston University
Deliverable due date:	31 June 2021
Actual delivery date:	29 November 2022
Dissemination level:	Public

Project Details

Project Acronym	WON
Project Title	Wideband Optical Networks
Call Identifier	H2020-MSCA-2018 Innovative Training Networks
Coordinated by	Aston University, UK
Start of the Project	1 January 2019
Project Duration	48 months
WON website:	https://won.astonphotonics.uk/
CORDIS Link	https://cordis.europa.eu/project/rcn/218205/en

WON Consortium and Acronyms

Consortium member	**Legal Entity Short Name**
Aston University	Aston
Danmarks Tekniske Universitet	DTU
VPIphotonics GmbH	VPI
Infinera Portugal	INF PT
Fraunhofer HHI	HHI
Politecnico di Torino	POLITO
Technische Universiteit Eidhoven	TUE
Universiteit Gent	UG
Keysight Technologies	Keysight
Finisar Germany GmnH	Finisar
Orange SA	Orange
Technische Universitaet Berlin	TUB
Instituto Superior Tecnico, University of Lisboa	IST

CONTENTS

ABBREVIATIONS

BDFA:	Bismuth-doped fibre amplifier
CAPEX:	Capital expenditure
CRF:	Corning Raman fibre
CUT:	Channel under test
DRA:	Discrete Raman amplifiers
EDFA:	Erbium-doped fibre amplifier
ISRS:	Inter-channel stimulated Raman scattering
MBT:	Multiband transmission
NF:	Noise figure
OSA:	Optical spectrum analyzer
OSNR:	Optical signal-to-noise ratio
PCE:	Power conversion efficiency
SMF:	Single mode fibre
SOA:	Semiconductor optical amplifier
TDFA:	Thulium-doped amplifier
UWB:	Ultra-wideband

LIST OF FIGURES

EXECUTIVE SUMMARY

The present scientific deliverable is a part of the Work Package 3 “Inline component design” of ETN project WON “Wideband Optical Network”, funded under the Horizon 2020 Marie Sklodowska-Curie scheme Grant Agreement 814276

This document provides an overview of Raman and Bismuth doped fibre amplifiers, designed and characterized for enabling multiband transmission (MBT). Here, we present a novel multistage Raman amplifier offering the potential of signal amplification over a bandwidth of 195 nm covering the E-, S, C-, and L-band of the optical window. The state-of-the-art Raman amplifier is based on a split-combine approach of the spectral band to minimize pump-to-pump and pump-to-signal overlapping. Our proposed amplifier showed an average gain of 14 dB and a maximum noise figure NF of 7.5 dB. Additionally, we demonstrate an E-band Bismuth-doped fibre amplifier (BDFA) with a maximum gain of 40 dB. The BDFA features a minimum NF of 4.6 dB. The power conversion efficiency (PCE) of the BDFA is 38% which is a record value for E-band BDFAs.

1. Introduction

The unprecedented demand for data with each passing year requires the design and development of new optical technologies potentially feasible for enabling high throughput data over the long term [1]. This has led the scientific communities to strategize different methodologies for both short as well as long-term solutions to meet these demands. Techniques such as subcarrier multiplexing [2] and high baud rate per channel [3] are cost-effective solutions requiring minimal infrastructural change. However, these are short-term solutions due to bandwidth limitations as we approach the nonlinear Shannon limit. Another interesting approach can be data transmission in the spatial domain (space division multiplexing) [4], [5]. The approach of space division multiplexing (SDM) is based on either transmission of data through multiple cores of fibre or transmission of higher order modes through a fibre, where the net data rate is an integral multiple of the number of cores and the number of modes of a given fibre. This technique is highly novel as the data rate can be increased to ~100 times the existing network capacity. However, the development of such an architecture requires expensive capital expenditure (CAPEX) and complex system integration when targeted towards a large scale deployment.

An alternative approach can be a full-scale exploitation of the optical windows in a single mode fibre (SMF), also known as multiband transmission (MBT) [6] covering the O-, E-, S-, C-, L- and U-band of the optical window, ~400 nm bandwidth. A combination of MBT with higher-order modulation formats can be a cost-effective network solution enabling full utilization of an already existing fibre infrastructure with minimal CAPEX. The MBT architecture can also be combined with SDM technology for maximum data throughput over an optical network.

However, deployment of MBT architecture requires the design and development of systems at both the core network and operator network for high data throughput. The existing optical communication technology utilizes only the C+L-band (1530-1625 nm) of the optical window. Moving from the conventional C-band towards MBT architecture necessitates the design and development of new transceivers, amplifiers, and ROADMS capable of operating in these unused spectral bands. Speaking particularly of amplifiers for MBT infrastructure [7], the existing erbium-doped fibre amplifier (EDFA) in the fibre network can support only the C- and L-bands [8] of the optical window. Hence, the

design and development of amplifiers capable of signal amplification in these unused spectral bands is a necessary step towards the establishment of MBT architecture. Amplification with rare-earth materials such as Bismuth, Thulium, and Praseodymium can be a good choice for signal amplification in for O-, E- and S-band with numerous experimental demonstrations showing the use of such amplifiers in transmission systems [9]–[12]. Another interesting amplifier enabling multiband (MB) signal amplification is the semiconductor optical amplifier (SOAs) with experimental demonstrations showing an extensive amplification of ~100 nm [13], [14] covering the C- and L-band of the optical window. The fibre optic parametric amplifier is also an interesting amplifier where a gain bandwidth of ~100nm has been demonstrated in [15].

Among the doped fibre amplifiers, Bi-doped fibre amplifiers (BDFAs) are the most flexible solution allowing to achieve gain from 1100-1800 nm. This spectral flexibility can be achieved by using different co-dopants in the core of the fibre and, thus, introducing different Bi-related active centres [16,17]. Recently, BDFAs showed great potential for wideband transmission [18]. However, the power conversion efficiency (PCE) of the amplifiers in the E-band are yet to be improved. Here we propose designs of the BDFAs with record PCE and Gain.

In addition to the abovementioned amplifiers, a separate category of an amplifier capable of ultra-wideband (UWB) signal amplification is the discrete Raman amplifiers (DRA). Recently, an experimental demonstration has shown an amplification bandwidth of 210 nm over the E-, S-, C- and L-bands, with a net gain of 15 dB and a maximum noise figure (NF) of ~8 dB, with dual-stage DRA [19]. In terms of maximum achievable gain, a record gain of 27 dB with an average NF of 5.8 dB using dual-stage DRA for C- and L-band has been reported in [20].

2. Multistage Discrete Raman amplifier

2.1 Design and characterization

The schematic of the proposed multistage DRA is illustrated in Figure 1(a). The amplifier design is based on a split-combine approach of the spectral band where signals from 1410-1457 (E-band) and 1470-1605 nm (S-, C- and L-band) were split into two separate bands for independent amplification. The E-band signals were amplified using a newly developed fibre named Corning Raman fibre (CRF) of 8.25 km in length [21], [22], and the S-, C- and L-band signals were amplified in a dual-stage fashion with two inverse dispersion fibres of 7.5 km each. In total 11 pumps extending from 1325 to 1508 nm were used for the Ultra-wideband (UWB) amplification where, the E-band signals were pumped using 1325, 1345, and 1365 nm pumps with pump power values of 435, 276, and 168 mW. The S-, C- and L-band were amplified in two stages, where the S-band was amplified in stage 1 using 1365, 1385 and 1405 nm pumps with power values of 432, 297, 103 mW, and the C- and L-band signals were amplified in stage 2 with 1405, 1425, 1445, 1465, 1485 and 1508 nm pumps having pump power values of 289, 304, 269, 67 and 172 mW. The experimentally measured Raman gain coefficient of both the test fibres can be seen in Figure 1(b) with CRF having a peak Raman gain coefficient (g_r) of ~1.95 $W^{-1}km^{-1}$ and IDF with a peak Raman gain coefficient (g_r) of ~1.2 $W^{-1}km$. The CRF was chosen for the E-band signals as the E-band signals undergo higher loss and hence, it requires higher gain for compensation which can be provided using CRF as its Raman gain coefficient is larger as compared to that of IDF. For the S-, C-, and L-band, we use IDF, as previous studies have shown quality results with the use of IDF in a dual-stage DRA [19], [23].

The amplifier shown in Figure 1(a) was characterized using an E-, S-, C-, and L-band WDM comb. The WDM comprises 143x100 GHz (50 GHz bandwidth) spectrally shaped ASE channels covering the S-, C- and L-band from 1470 to 1605 nm and 3 narrow linewidth lasers at wavelengths of 1411, 1431, and 1451 nm and a PM-16QAM signal at 1457 nm to encapsulate a total bandwidth of 195 nm.

The S-band channels were generated using a supercontinuum source and a commercial waveshaper to provide channel shaping and flattening followed by a commercial thulium-doped amplifier (TDFA) operating in the wavelength range of 1470-1520 nm. The S-band comb was then combined with a flat channelized C- and L-band ASE comb extending from 1530-1605 nm generated using two C- and L-band commercial EDFAs and two equalizers per band for equalization. This S-, C- and L- grid was then coupled with the four E-band signals to form an E-, S- C- and L-band WDM grid [Figure 2(a)]. For the E-band due to the unavailability of any commercial ASE source and equalizer for channel shaping and flattening we had to use 3 independent laser diodes and a modulating signal covering the target bandwidth. Nevertheless, we managed to insert the signals at the extreme ends of the targeted wavelengths to validate the performance of the multistage DRA. The generated signals were then transmitted through 70 km long SMF before being amplified in the multistage DRA. This setup was particularly chosen to perform a standalone experiment for future transmission, where the effects of inter-channel stimulated Raman scattering (ISRS) and wavelength-dependent losses are dominant. In the dual-stage part of the amplifier guard bands of +/- 2nm in the proximity of 1485 nm and +/- 3nm at 1508 nm were inserted to prevent a signal overlap with 1485 and 1508 nm pumps in the DRA stage, the technique is well explained in the work [24].

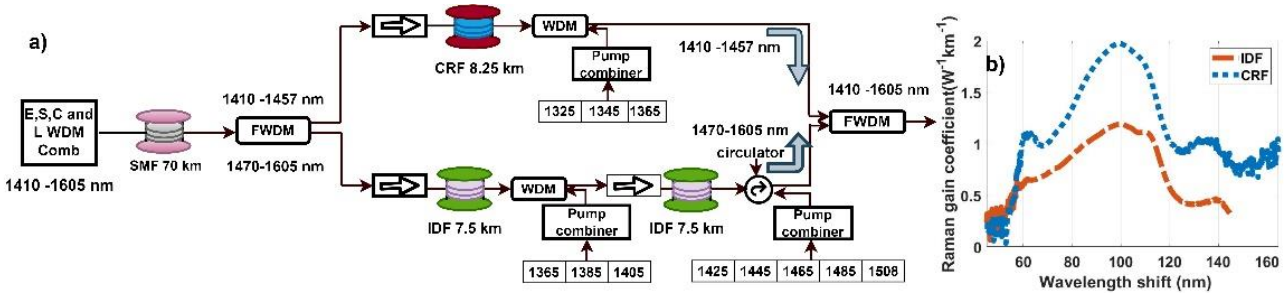

Figure 1: a) Schematic of the multistage DRA b) Raman gain coefficient of IDF and CRF gain fibres.

2.2 Results and discussion

Figure 2(a-c) illustrates the optical spectra at the SMF input section, output section, and the amplified spectrum after the multistage DRA. The signals in the S-band region (1470-1520 nm) have a higher noise floor than the C- and L-band signals (1530-1605 nm). This is due to the high noise figure (NF) of the TDFA, and high waveshaper loss used for the S-band grid generation. Also, a slight tilt of +/-1 dB in the S-band input spectrum (Figure 2(a)) was obtained due to the wavelength-dependent loss of the passives used during the signal combination. The peaks observed in the vicinity of the S-band (Figure 2 (c)) are the Rayleigh backscattered spectra of 1465, 1485, and 1508 nm pumps and the zoomed-in spectra of these pumps are shown in Figure 2 (d-e). As explained in the previous section, appropriate guard bands of +/- 2nm and +/- 3 nm were kept for 1485 and 1508 nm pumps to prevent overlapping with the corresponding signals [24]. The output optical spectrum in Figure 2(c) has a higher tilt in the S-band particularly towards the lower wavelengths near 1470 nm due to the power limitations of the pumps and also due to the availability of the commercial pumps at only specific wavelengths. The maximum channel ripple for C- and L-band signals was +/- 1.5 dB across the entire bandwidth.

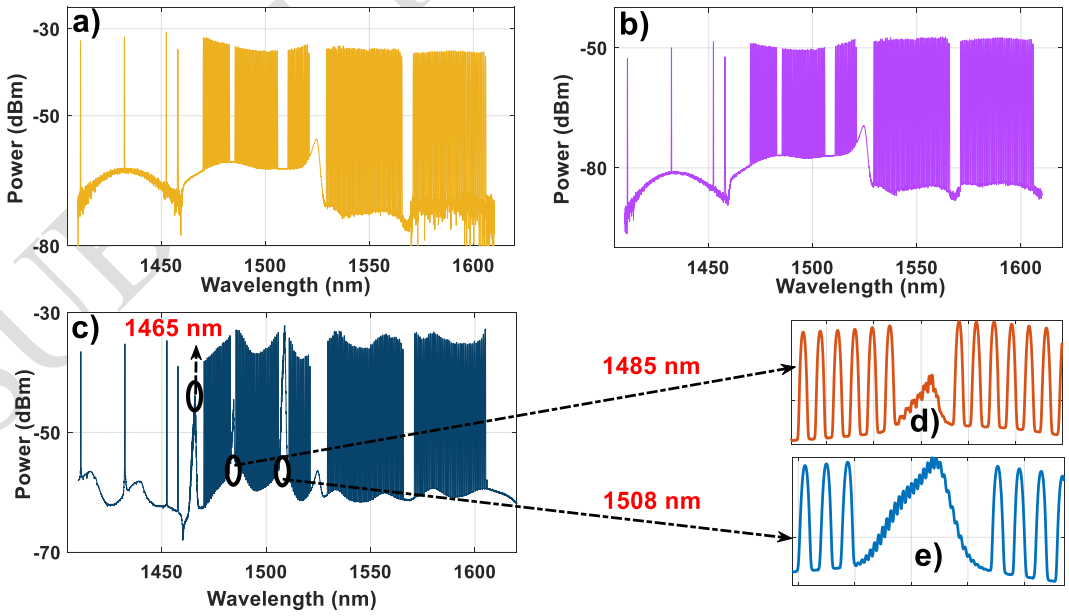

Figure 2:WDM optical spectrum of the E-, S-, C- and L-band a) input to 70 km SMF b) output from 70 km SMF c) output spectrum from the multistage DRA; Rayleigh backscattered spectrum of d) 1485 and e) 1508 nm pumps.

Figure 3 (a-b) shows the Gain and NF and the output optical signal-to-noise ratio (OSNR) after the multistage DRA. An average gain of 14 dB (orange lines with circle markers) with a maximum NF of 7.5 dB (grey line with circle marker) was obtained across the entire bandwidth of 195 nm. The emphasis of the characterization was not to obtain a flat gain but rather to compensate for the power loss incurred after 70km of transmission. This resulted in a tilted gain profile due to the tilted input power profile (Figure 2(b)) at the input stage of the DRA. For the E-band signals, an average gain of ~15 dB was necessary to compensate for the power loss after the 70 km SMF propagation. An average gain of ~16 dB was required to compensate for the loss of the S-band signals. This is mainly due to the higher SMF loss window in the S-band region and ISRS power transfer in the SMF and stages of the dual-stage DRA. Similarly, towards the C- and L-band an average gain of ~13 dB was required to compensate for the SMF loss. The net gain for the C- and L-band was lower as compared to the E- and S-band due to the lower power loss and additional benefits of ISRS power transfer from the E- and S-band signals.

The NF for the E-band channels has an average value of ~7 dB. However, a slight increment in the NF can be expected with a fully loaded channelized E-band spectrum due to an increased power spectral density. The overall NF of the S-, C-, and L-bands is due to the dual-stage architecture adopted here. A higher NF for the S-band signals is due to the power loss in the SMF, as well as due to the high thermal noise generated by the neighboring 1465, 1485, and 1508 nm pumps. A slightly lower value of NF can be seen with a value of ~ 6 dB across the 1530-1605 nm signals, which is due to ISRS power transfer from the S-band signals to these wavelengths and also due to the low loss at these wavelengths. Note that the NF in the E- and S-band can be improved by replacing CRF and IDF with a fibre having a lower E-, S-band loss and implementing a dual stage amplification for E- and S-bands [24], with appropriate pump wavelengths and powers.

The output OSNR shown in Figure 3b corresponds to the OSNR measured at the output stage of the multistage DRA. The measurements were performed by loading 30 GBaud PM-16 QAM signals and measuring the values at an interval of 10 nm. For the OSNR measurements in the S-, C- and L-band regions, two side channels across the channel under test (CUT) were turned off and the corresponding OSNR was measured using the 3–point method [25] at a noise bandwidth of $\Delta B = \frac{C}{\lambda^2} * \Delta\lambda$ [26] where, C is the speed of light, $\Delta\lambda$ is the optical spectrum analyzer (OSA) resolution bandwidth which is 0.1 nm and λ is the wavelength of CUT. For the E-band signals, there was no requirement for channels to be turned off due to sufficient channel spacing between the test channel and the adjacent signals.

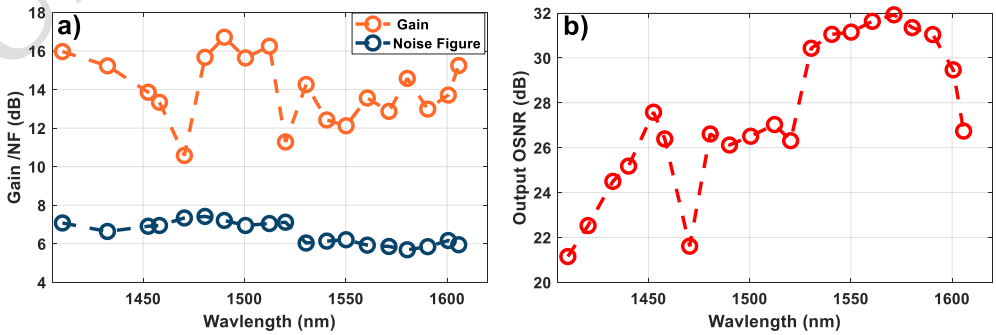

Figure 3:Multistage Raman amplifier characterization wavelength vs a) Gain/ Noise figure b) amplifier output OSNR.

Our experimental characterization for the output OSNR shows a lower value towards the E- and S-band channels. The degradation in the output OSNR in the E- and S-band is due to the high NF of the DRA in this region. For the S-band signals, in addition to the DRA NF, the OSNR degradation is also partly due to the low input OSNR of the S-band signals arising from the high NF of the TDFA and high insertion loss of the WSS used for the channel shaping and flattening. The minimum value of NF for the S-band signals was ~21 dB for 1470 and 1410 nm. For the C- and L-band signals (1530-1605 nm), an improved OSNR was obtained, with its values in the range of 27 to 31 dB. This improved OSNR for C- and L-band signals can be attributed to the low NF of the DRA, power gain due to the ISRS power transfer from S- and E-band signals, and the low noise floor of the input ASE grid (Figure 2(a)).

3. Bismuth-doped fibre amplifier

The schematic of the bismuth-doped fibre amplifier is presented in Fig. 4. The developed amplifier consists of TFF-WDMs used for multiplexing and demultiplexing of radiation at pump (1250-1320 nm) and signal (1330-1500 nm) wavelengths. The TFF-WDMs have very steep and flat transmission and reflection bands that allow to achieve consistent loss over the whole operation bandwidth. Two isolators centred at 1320 nm were used to avoid back reflection of radiation to the pump diodes, and two 1440 nm isolators were used for unidirectional transmission of the signal. Two LD and TEC controllers were used to control temperature and output power of the pump laser diodes. The Bi-doped germanosilicate fibre used in this work is fabricated in FORC using the conventional MCVD-solution doping technique and has the length of 173 m. The fibre has a 6 µm core diameter and 125 µm cladding diameter. The refractive index difference (Δn) between the core and cladding is around 0.004. The fibre core consists of 95 mol% SiO2, 5 mol% GeO2 and <0.01 mol% of bismuth. The cutoff wavelength (λc) of the fibre is measured to be around 1000 nm.

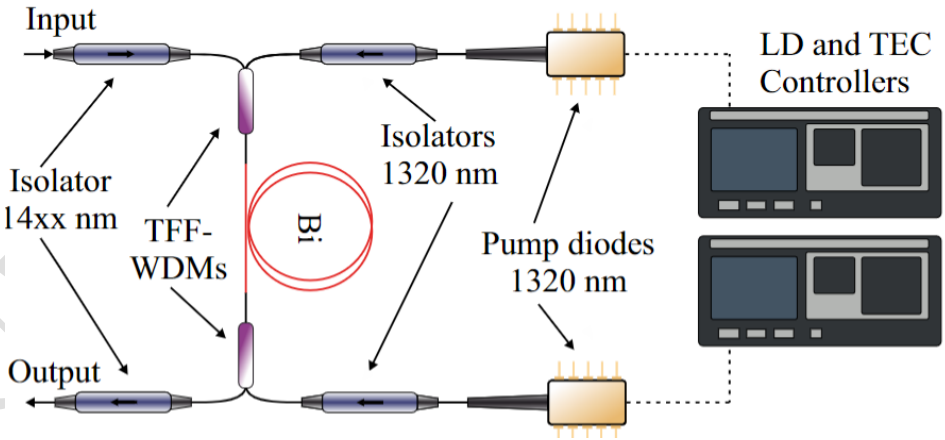

Figure 4: Schematic of BDFA based on 6 µm core diameter fibre

As the first step, the performance of the developed BDFA for a bi-directional pumping scheme and seven different signal powers in the range from -25 to 5 dBm with a step of5 dB is characterised. The gain and NF for the bi-directional pumping scheme and seven different signal levels are depicted in Figure5. Figure 5(a) shows recorded spectra of the gain for all seven input signal powers and 1 W total pump power equally split between forward and backward pump lasers. The amplifier features a maximum gain of 39.8 dB for -25 dBm input signal power. The maximum gain substantially decreases

to 20.8 dB with the increase of input signal to 5 dBm. On the other hand, the 3 dB bandwidth of the gain rises with increase of the input signal from 30.9 nm to 73.6 nm for -25 dBm and 5 dBm input signal powers, respectively. Figure 5(b) shows the spectra of NF for seven different input power signals. The minimal NF of 4.58 dB is achieved with -25 dBm pump at 1468 nm. The NF rises up to 5.27 dB with increase of input signal power to 5 dBm. The NF has a predominantly linear trend with wavelength, substantially decreasing from the short to the long wavelength side. However, the NF dependency flattens by reaching 1470 nm.

The dependence of both gain and NF on the pump power are also recorded and shown in Figure 5(c) and 5(d), respectively. These dependencies are measured for all seven input signal powers and wavelengths, however, the dependencies at only 1430 nm are presented as they all follow the same pattern. The predictable performance of the amplifier is observed: rise of the gain and reduction of the NF with an increase of pump power. The gain curves follow a well-pronounced logarithmic trend, and NF ones, on the other hand, are inverse logarithmic. The minimal pump power of 50 mW allowed to already achieve 5 dB gain for 5 dBm signal and 20 dB gain for -25 dBm signal, NF in this case was substantially higher with 10 dB and 7.5 dB for 5 dBm and -25 dBm signals, respectively.

Another important characteristic of an optical amplifier is optical PCE. The measured PCE dependence on both total pump power and input signal power at the 1430 nm is represented as a colour map in Figure 5(e). The maximum PCE is 38% which is the record value for Bi-doped fibre amplifiers. This value is observed at a maximum signal power of 5 dBm. The PCE saturates significantly with increase of pump power above a pump power of around 250 mW. The spectral dependence of PCE for different input power signals is presented in Figure 5(f). The decrease of input signal power significantly worsens the PCE to just 3.6% for a -25 dBm signal due to lower interactions between the radiation of the signal with Bi-related active centres in the core of the fibre and predominant amplification of spontaneous emission. However, it is important to note that generally amplifiers utilised for DWDM systems work at high total input signal powers (0-10 dBm) due to a high number of channels, and thus, the amplifier should maintain high PCE even if individual channels have low power. An additional experiment was performed with 6 channels in the E-band (1410, 1430, 1440, 1450, 1470, and 1490 nm) with total input power of 5 dBm. The PCE of the amplifier was calculated and was the same 38%.

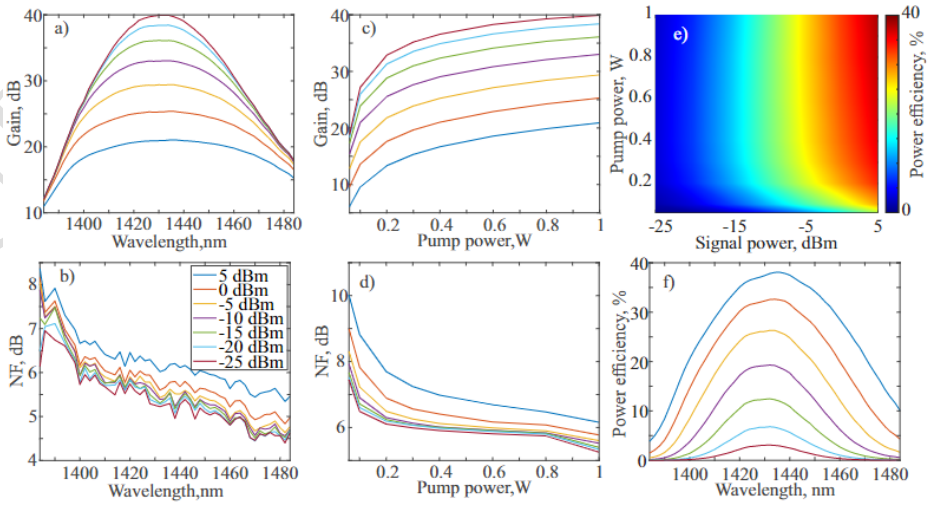

Figure 5: Spectral dependencies of BDFA gain (a) and NF (b) for seven input signal powers and pump power of 1 W; gain (c) and NF (d) dependencies on the pump power for seven input signal powers at 1430 nm; e) colour map of the PCE for depending from both input signal and pump powers; f) spectra of power efficiencies for seven input signal powers

Another remark should be made regarding achieved PCE of 38% which is the record value for Bi-doped fibre amplifiers. Most importantly, this value is almost twice as high as the PCE of L-band EDFAs which is typically around 20% [27]. It is also higher than that of C-band EDFAs pumped at 978 nm with 33% PCE, however, it is less than EDFAs pumped at 1480 nm with 50 % PCE [28]. Nevertheless, such a high PCE along with 40 dB Gain and 4.6 dB NF shows great potential for BDFAs to be used for extending the current optical communication bandwidth while keeping relatively low power consumption of the line, and, potentially, even better power consumption that L-band amplifiers offers which are currently being deployed.

Additionally, another BDFA was designed based on the same schematic and similar fibre with shorter length of 150 m. This BDFA has maximum gain of 35 dB, minimal NF of 5.1 dB and PCE of 25%. As the behaviour of the amplifier does not significantly differ from the BDFA presented in this report, we will not present the detailed investigation of that BDFA here. The details of this amplifier will be reported elsewhere.

4. Conclusion

In this deliverable, we proposed an in-house multistage discrete Raman amplifier offering a signal amplification of 195 nm covering the E-, S-, C-, and L-band of the optical window. The developed amplifier was characterized using 146 ASE dummy channels and modulating signal, for Gain and NF measurements, and a PM-16QAM modulating signal of 30 GBaud was used for the amplifier output OSNR measurements. Our experimental results show an average gain of 14 dB with a maximum NF of 7.5 dB across the entire bandwidth. The output OSNR after the amplification stage has a range of 27 to 31 dB for the C- and L-band signal whereas, for E- and S-band an average OSNR of ~26 dB was obtained with its minimum value being ~21 dB from 1410 and 1470 nm signals. Based on our experimental results we can conclude that the discrete Raman amplifier is a potential candidate for signal amplification in MBT systems. Further improvement in the performance of a multistage DRA can be achieved with the availability of commercial pumps at appropriate wavelengths and powers coupled together with low loss and high Raman gain fibres in the region of operation.

In addition, we developed a single-stage E-band bismuth-doped fibre amplifier with, to the best of our knowledge, record parameters for an E-band BDFA of 40 dB gain and 4.5 dB NF. The amplifier was characterized in terms of gain, NF, 3 dB bandwidth, and power conversion efficiency. Moreover, the developed amplifier has comparable performance in terms of power conversion efficiency with commercially available EDFAs. Additional optimization of the amplifier fibre length might potentially increase the power conversion efficiency while keeping moderate gain and NF. This might ensure similar costs per bit by utilizing multi-band transmission for traffic operators.

Future work includes validation of the multistage discrete Raman amplifier over a high-speed coherent transmission system and a combination of E-band BDFAs with Raman for wideband coherent transmission.

5. REFERENCES

[1] P. J. Winzer, D. T. Neilson, and A. R. Chraplyvy, “Fiber-optic transmission and networking: the previous 20 and the next 20 years [Invited],” *Opt. Express*, vol. 26, no. 18, p. 24190, 2018, doi: 10.1364/oe.26.024190.

[2] Y. Zhang, M. O’Sullivan, and R. Hui, “Digital subcarrier multiplexing for flexible spectral allocation in optical transport network,” *Opt. Express*, vol. 19, no. 22, p. 21880, 2011, doi: 10.1364/oe.19.021880.

[3] S. A. Li *et al.*, “Enabling Technology in High-Baud-Rate Coherent Optical Communication Systems,” *IEEE Access*, vol. 8, pp. 111318–111329, 2020, doi: 10.1109/ACCESS.2020.3003331.

[4] D. J. Richardson, J. M. Fini, and L. E. Nelson, “Space-division multiplexing in optical fibres,” *Nat. Photonics*, vol. 7, no. 5, pp. 354–362, 2013, doi: 10.1038/nphoton.2013.94.

[5] B. J. Puttnam, G. Rademacher, and R. S. Luís, “Space-division multiplexing for optical fiber communications,” *Optica*, vol. 8, no. 9, p. 1186, 2021, doi: 10.1364/optica.427631.

[6] A. Ferrari *et al.*, “Assessment on the Achievable Throughput of Multi-Band ITU-T G.652.D Fiber Transmission Systems,” *J. Light. Technol.*, vol. 38, no. 16, pp. 4279–4291, 2020, doi: 10.1109/JLT.2020.2989620.

[7] L. Rapp and M. Eiselt, “Optical Amplifiers for Multi – Band Optical,” *J. Light. Technol.*, vol. 40, no. 6, pp. 1579–1589, 2022.

[8] A. A. Al-Azzawi *et al.*, “Gain-flattened hybrid EDFA operating in C + L band with parallel pumping distribution technique,” *IET Optoelectron.*, vol. 14, no. 6, pp. 447–451, 2020, doi: 10.1049/iet-opt.2020.0072.

[9] J. Mirza, S. Ghafoor, N. Habib, F. Kanwal, and K. K. Qureshi, “Performance evaluation of praseodymium doped fiber amplifiers,” *Opt. Rev.*, vol. 28, no. 6, pp. 611–618, 2021, doi: 10.1007/s10043-021-00706-z.

[10] M. M. Kozak, R. Caspary, and W. Kowalsky, “Thulium-doped fiber amplifier for the S-band,” *Proc. 2004 6th Int. Conf. Transparent Opt. Networks*, vol. 2, pp. 51–54, 2004, doi: 10.1109/icton.2004.1361967.

[11] Y. Wang, N. K. Thipparapu, D. J. Richardson, and J. K. Sahu, “Ultra-Broadband Bismuth-Doped Fiber Amplifier Covering a 115-nm Bandwidth in the O and e Bands,” *J. Light. Technol.*, vol. 39, no. 3, pp. 795–800, 2021, doi: 10.1109/JLT.2020.3039827.

[12] A. Donodin *et al.*, “Bismuth doped fibre amplifier operating in E- and S- optical bands,” *Opt. Mater. Express*, vol. 11, no. 1, p. 127, 2021, doi: 10.1364/ome.411466.

[13] J. Renaudier *et al.*, “100nm Ultra-Wideband Optical Fiber Transmission Systems Using Semiconductor Optical Amplifiers,” in *European Conference on Optical Communication, ECOC*, 2018, pp. 1–3. doi: 10.1109/ECOC.2018.8535354.

[14] J. Renaudier *et al.*, “First 100-nm Continuous-Band WDM Transmission System with 115Tb/s Transport over 100km Using Novel Ultra-Wideband Semiconductor Optical Amplifiers,” in *European Conference on Optical Communication, ECOC*, 2017, no. 1, pp. 1–3. doi: 10.1109/ECOC.2017.8346084.

[15] J. D. Marconi, J. M. Chavez Boggio, H. L. Fragnito, and S. R. Bickham, “Nearly 100 nm bandwidth of flat gain with a double-pumped fiber optic parametric amplifier,” *Opt. InfoBase Conf. Pap.*, pp. 7–9, 2007.

[16] I. Bufetov, M. Melkumov, V. Khopin, *et al*., “Efficient Bi-doped fiber lasers and amplifiers for the spectral region 1300-1500 nm”, in Fiber Lasers VII: Technology, Systems, and Applications, International Society for Optics and Photonics, vol. 7580, 2010, p. 758 014.

[17] S. Firstov, K. Riumkin, A. Khegai, et al., “Wideband bismuth-and erbium-codoped optical fiber amplifier for c+ l+ u-telecommunication band”, Laser Physics Letters, vol. 14, no. 11, p. 110 001, 2017.; 12; 11.

[18] Ososkov, Yan, *et al*. "Pump-efficient flattop O+ E-bands bismuth-doped fiber amplifier with 116 nm–3 dB gain bandwidth." Optics Express 29.26 (2021): 44138-44145

[19] P. Hazarika, M. Tan, A. Donodin, I. Phillips, P. Harper, and W. Forysiak, “210 nm E, S, C and L Band Multistage Discrete Raman Amplifier,” 2022.

[20] S. Liang *et al.*, “High Gain, Low Noise, Spectral-Gain-Controlled, Broadband Lumped Fiber Raman Amplifier,” *J. Light. Technol.*, vol. 39, no. 5, pp. 1458–1463, 2021.

[21] P. Hazarika, M. Abu-Romoh, M. Tan, L. Krzczanowicz, and T. T. Nguyen, “Impact of Chromatic Dispersion in Discrete Raman Amplifiers on Coherent Transmission Systems,” pp. 5–7.

[22] M. J. Li, S. Li, and D. A. Nolan, “Nonlinear fibers for signal processing using optical Kerr effects,” *J. Light. Technol.*, vol. 23, no. 11, pp. 3606–3614, 2005, doi: 10.1109/JLT.2005.857768.

[23] M. Asif Iqbal, L. Krzczanowicz, I. Phillips, P. Harper, and W. Forysiak, “150nm SCL-band transmission through 70km SMF using ultra-wideband dual-stage discrete raman amplifier,” in *Optical Fiber Communication Conference (OFC)*, 2020, pp. 1–3. doi: 10.1364/OFC-2020-W3E.4.

[24] M. A. Iqbal *et al.*, “Impact of pump-signal overlap in S+C+L band discrete Raman amplifiers,” *Opt. Express*, vol. 28, no. 12, p. 18440, 2020, doi: 10.1364/oe.392258.

[25] “OSNR | ROADM | Signal Power | EXFO.” https://www.exfo.com/en/resources/blog/new-iec-standard-osnr-measurements/ (accessed Jun. 02, 2022).

[26] R. Emmerich *et al.*, “Enabling S-C-L-band systems with standard C-band modulator and coherent receiver using nonlinear predistortion,” *J. Light. Technol.*, vol. 40, no. 5, pp. 1360–1368, 2021, doi: 10.1364/ofc.2021.f4d.7.

[27] Li Qian and Ryan Bolen. Erbium-doped phosphosilicate fiber amplifiers: a comparison of configurations for the optimization of noise figure and conversion efficiency. In Photonic Applications in Devices and Communication Systems, volume 5970, page 59702V. International Society for Optics and Photonics, 2005

[28] RI Laming, JE Townsend, DN Payne, F Meli, G Grasso, and EJ Tarbox. High-power erbium-doped-fiber amplifiers operating in the saturated regime. IEEE Photonics technology letters, 3(3):253–255, 1991.